Magnetic map of Mn-based thin films on Ni/Cu

B. R. Malonda-Boungou* and B. M'Passi-Mabiala
Groupe de Simulations Numériques en Magnétisme et Catalyse, Département de Physique, Faculté des Sciences, Université Marien Ngouabi, PB 69 Brazzaville, Congo

A. Debernardi
Laboratorio Nazionale MDM, CNR-INFM, Via C. Olivetti 2, Agrate Brianza, 20041 Milano, Italy

S. Meza-Aguilar
Escuela de Ciencias Fisico-Matematicas, Universidad Autonoma de Sinaloa, Bldv. De las Americas y Universitarios, Culiacán, CP 80010 Sinaloa, Mexico

C. Demangeat
Institut de Physique et Chimie des Matériaux de Strasbourg, 23 rue du Loess, F-67034 Strasbourg, France
(Received 23 September 2009; revised manuscript received 4 December 2009; published 8 January 2010)

Ab initio density-functional theory in generalized gradient approximation is used to perform calculations on the magnetic structure of Mn thin films and Mn-Ni ordered surface alloys on Ni/Cu. For the Mn monolayer on Ni(001), Ni(011), and Ni(111), we found that the ground state corresponds to an antiferromagnetic coupling between Mn atoms. Ni subsurface atoms adjacent to Mn surface display two different values ($0.26\mu_B$ and $0.13\mu_B$) of the magnetic moment in the (111) crystallographic face. For the ordered $Mn_{0.5}Ni_{0.5}$ monolayer on Ni a ferromagnetic configuration has been obtained. At variance, for the ordered $Mn_{0.5}Ni_{0.5}$ two-layers thick on Ni an antiferromagnetic coupling between Mn atom nearest-neighboring positions are depicted for the (001) and (011) crystallographic faces whereas it is ferromagnetic for (111) one. Ni magnetic moments at surface alloy are killed ($-0.04\mu_B$). Mn overlayer and 1–2 ML surface alloy always present a large rippling, in qualitative agreement with experimental measurements [M. Wuttig and C. C. Knight, Phys. Rev. B **48**, 12130 (1993); M. De Santis, V. Abad-Langlais, Y. Gautier, and P. Dolle, Phys. Rev. B **69**, 115430 (2004)].

DOI: 10.1103/PhysRevB.81.024402 PACS number(s): 75.70.−i, 71.15.Mb, 68.47.De, 82.45.Mp

I. INTRODUCTION

In recent years, in the solid-state community it has become popular to use the term spintronics to denote materials or devices whose interesting physical properties are determined by the spin of electrons rather than the electron charge. In this context a particular effort has been devoted to study magnetic nanostructures due the specular magnetic properties displayed by surface nanoaggregates as an effect of the reduction in the dimensionality and of the coordination number. Vaz *et al.*[1] reviewed the results of recent experimental and theoretical studies of well-characterized epitaxial structures based on Fe, Co, and Ni to illustrate how intrinsic fundamental properties such as the magnetic exchange interactions, magnetic moment, and magnetic anisotropies change markedly in ultrathin films as compared with their bulk counterparts, and to emphasize the role of atomic-scale structure, strain, and crystallinity in determining the magnetic properties. The study of the magnetic moment of thin fcc Ni films, particularly for the Ni/Cu interface, has been considered in some detail by several authors fuelled in large measure by the discrepancy in the reported observation of the Ni magnetic moment with film thickness.

Among the elements that are candidate to be used into novel spintronic devices, Mn has attracted considerable interest due to its high magnetic moment. However, in order to be useful for spintronic applications, Mn atoms must be stabilized ferromagnetically, e.g., by coupling with a ferromagnetic substrate. To provide a valuable solution to this problem a specific effort was devoted to study two-dimensional Mn monolayer in contact with metallic substrates.[2,3] Surface atoms display not only an enhanced magnetization due to the reduced coordination but, in general, also present a significant outward relaxation that may contribute to enhance their magnetic moment. It is therefore of paramount importance to establish the morphologic structure of thin films of Mn on ferromagnetic substrates such as Fe, Co, of Ni, and if these Mn films are ferromagnetic (FM) or antiferromagnetic (AF) coupled with the substrate.

Usually, thick layers of ferromagnetic element are epitaxially grown on nonmagnetic substrate of similar lattice parameter, as is the case of Ni and Co magnetic layers that are grown epitaxially on Cu substrate. Thin (Mn) magnetic layers are then grown on the top of these heterostructures (Ni/Cu). The Cu seed layer do not affects the Mn overlayers because the Ni substrate is thick enough. However the (Cu) substrate can indirectly influence the magnetic of surface layer since it determines the lattice parameter in the plane parallel to the surface.

The Mn/Co/Cu(001) structure has been experimentally studied by O'Brien and Tonner,[4] showing that Mn layers on top of ferromagnetic Co display an high-spin state. Later Choi and co-workers,[5] on the basis of Kerr effect measurements and low-energy electron-diffraction data, suggested the existence of a Mn-Co surface alloy with $c(2\times2)$ ordered structure. Both works provide evidence that when the thickness of Mn layer is larger than one monolayer (ML) the Mn ferromagnetic order decrease dramatically. Recently, Chan

and co-workers[6] have deposited 6 MLs of Co on Cu(001) surface, and then they have deposited a 4 ML Mn layer on top of Co MLs with a mask placed in front of the sample. Although the signal obtained by x-ray magnetic circular dichroism (XMCD) was relatively weak, the ferromagnetic order between Co and Mn layers was clearly detected. Theoretical investigations on the Mn/Co/Cu(001) system confirmed that the $Mn_{0.5}Co_{0.5}$ alloy is the state with minimum energy.[7,8]

Here we carry out a systematic study of the Mn/Ni/Cu system using the plane-wave self-consistent field (PWSCF) code[9,10] with pseudopotential (based on the spin-resolved density-functional theory), for (001), (111), and (011) crystallographic faces. This code takes into account the optimization of the geometry. Our research is motivated by the availability of a considerable amount of experimental results of Mn films on Ni substrates.[11–15] Wuttig *et al.*[11] studied by low-energy electron diffraction (LEED) Mn-Ni film epitaxially grown on Ni(001) by deposition of 3–4 Mn MLs above 550 K, finding an ordered Mn-Ni films with tetragonal structure with a pronounced corrugation of 0.30 ± 0.02 Å at the Mn-Ni film surface (Fig. 1). Later, a comparative investigation on Mn films grown on Cu(001) and Ni(001) substrates was performed by O'Brien and Tonner[16] by using XMCD and soft x-ray absorption spectroscopy. The authors observed a large buckling of surface atoms on both substrates while a ferromagnetic order was detected only on Mn film on Ni substrate. For both Mn/Cu and Mn/Ni systems, the same authors also measured an enhancement of the magnetic moment of Mn atoms, due to the localization of the Mn $3d$ orbitals. They concluded that Mn is in high-spin d^5 state and that the buckling originates from the increasing atomic radii of Mn due to the change in electronic structure.

In a recent work, De Santis and co-workers[15] have shown, by using quantitative x-ray-diffraction analysis, that the deposition of about half a ML on Ni(110) at 440 K, produces an ordered $c(2\times2)$ phase where the deposited atoms occupy the substitutional sites of the outermost layer with a checkboard arrangement. This surface Mn-Ni ML presents a large rippling, with Mn shifted outward. This $c(2\times2)$ ordered structure is observed over a large temperature range (from room temperature to above 440 K). It is expected that a high-spin state of Mn is associated with this structure by analogy with similar surface alloys.

Experimentally, it is difficult to achieve a perfect pseudomorphic growth. In fact, in general, at finite temperature, the growth of films is affected by two phenomena: (i) the diffusion of atoms at the surface, which may lead to formation of clusters and (ii) the interdiffusion of the adatoms into the substrate, which may lead to the formation of bulk alloys or clusters of film atoms covered by substrate atoms.

More recently, Bala *et al.*[17] have focused on electronic and magnetic properties of nanosystems of early $3d$ transition metals. It has been noted that for systems such as MLs of Mn, the smaller values of equilibrium nearest-neighbor distance (d_{nn}) favor ferromagnetic ordering while larger values favor antiferromagnetic ordering. Through *ab initio* density-functional calculations on a Mn monolayer deposited on Fe(001) to which a top layer of O is added, Zenia *et al.*[18] have investigated the effect of oxidation on the Mn-Fe magnetic coupling. The clean Mn surface is found to be in an in-plane antiferromagnetic order with moments of $3.98\mu_B$ and $-4.39\mu_B$ on the two inequivalent atoms, the subsurface Fe moments being smaller than in the bulk case. Structural relaxation in the clean surface case yields a small buckling on the Mn overlayer as result of different couplings between Mn moments and Fe substrate ones.

The purpose of this work is the exploration and the comparison of the magnetic maps displayed by epitaxial Mn thin films and Mn-Ni surface alloys (in the 1–2 ML range) on Ni thick films, that are grown epitaxially on Cu substrates, with (001), (111), and (011) crystallographic orientations. We are not aware of any comparative *ab initio* calculations, with geometry optimization, for these systems. The manuscript is organized as follows. In Sec. II we comment on the computational model. In Secs. III and IV we present our results and a discussion, respectively, for Mn-based systems on Ni substrate: Mn monolayer and Mn-Ni ordered surface alloy (one- and two-layers thick) on a Ni substrate. Section V is devoted to the summary.

II. COMPUTATIONAL MODEL

Spin-polarized calculations have been carried out on Mn/Ni epitaxially grown on fcc Cu in [001], [111], and [011] directions (chosen as the z Cartesian axis), by using the pseudopotential PWSCF code.[10] The experimental lattice parameter of fcc Cu (=3.614 Å) is used because the Ni are growing epitaxially on nonmagnetic Cu substrate. Ni has a smaller lattice parameter as Cu (Ref. 1) so that it is necessary to carry out relaxation calculations in the z direction with Cu lattice parameter in the plane.

The fcc Ni clean surface, Mn metallic overlayer, Mn-Ni ordered alloy one-layer thick and Mn-Ni ordered alloy two-layers thick on fcc Ni [for (001), (111), and (011) crystallographic faces] are modeled, using the repeated slab geometry.[19] All these systems are modeled by a 13-layer slab consisting of (i) 13-layers fcc Ni film for the clean surface, with one atom per layer; (ii) 11 layers of Ni atoms surrounded at each surface by a Mn monolayer; (iii) 11 layers of Ni surrounded at each surface by a Mn-Ni ordered alloy, one monolayer thick; (iv) nine layers of Ni atoms surrounded at each surface by a Mn-Ni ordered alloy, two-layers thick. The films are separated by five layers of vacuum, i.e., the distance between the two films in the periodically repeated cell is 9.03 Å (17.06 a.u.). This empty space is sufficient to prevent interaction between slabs which is controlled through vanishing dispersion in the direction perpendicular to the slab and vanishing charge in the central layer of the empty space. The calculations are performed with two inequivalent atoms per layer for the Mn overlayer and for 1–2 ML ordered $Mn_{0.5}Ni_{0.5}$ alloy on fcc Ni.

In our calculation we first compute the solution of the self-consistent Kohn-Sham equations which describe a valence electron in the potential created by the periodic lattice of pseudonuclei (described by ultrasoft pseudopotentials generated by using the scheme proposed by Vanderbilt[20]) and by all the other valence electrons, and then we determine the forces acting on each atom. Forces and stress tensor are ob-

TABLE I. Magnetic moments (in μ_B) and Δz interlayer spacings (Å) with respect to the previous layer located in the bottom, in the case of a clean Ni surface for (001), (111), and (011) crystallographic faces. The center of slab is noted by 0.00.

	(001)		(111)		(011)	
	Δz (Å)	μ (μ_B)	Δz (Å)	μ (μ_B)	Δz (Å)	μ (μ_B)
Ni_1	1.64	0.75	1.97	0.71	1.07	0.81
Ni_2	1.73	0.67	2.00	0.70	1.29	0.69
Ni_3	1.71	0.66	2.01	0.66	1.22	0.67
Ni_4	1.71	0.64	2.00	0.65	1.22	0.67
Ni_5	1.71	0.66	2.00	0.66	1.24	0.66
Ni_6	1.71	0.66	2.01	0.66	1.23	0.69
Ni_7	0.00	0.65	0.00	0.66	0.00	0.64

tained from the Hellmann-Feynman theorem. The equilibrium geometry of the system is obtained by the condition that the forces acting on individual nuclei vanish. This self-consistent cycle is repeated until complete equilibrium geometry is obtained.

For (001), (111), and (011) crystallographic faces, the relaxation is only performed on the [001], [111], and [011] directions, respectively, taken as z axis. The plane-wave basis set is determined by a 35 Ry (476.20 eV) kinetic-energy cutoff while a 560 Ry (7619.2 eV) cutoff was used for the augmentation density. We used generalized gradients of GGA-PW-91 functional.[21] The ionic degrees of freedom are relaxed using a conjugate gradient minimization scheme until all components of all forces are smaller than 10^{-3} Ry/a.u. Brillouin-zone integrations were performed using $(12\times12\times2)$ grids of special points.

For the majority ($\uparrow$) and minority ($\downarrow$) electronic spins we have computed the density of states projected on atomic orbital (PDOS). For each atom we have integrated the PDOS of both spins, up to the Fermi energy. The magnetization in each atom is obtained by the difference PDOS($\uparrow$) $-$PDOS($\downarrow$). The sum PDOS($\uparrow$)+PDOS($\downarrow$) gives the contribution of each atom to the density of states of valence electrons. The total number of electrons per cell computed in this way has a numerical error of 0.4% that gives an estimation of the numerical accuracy of the magnetization moment per atom.

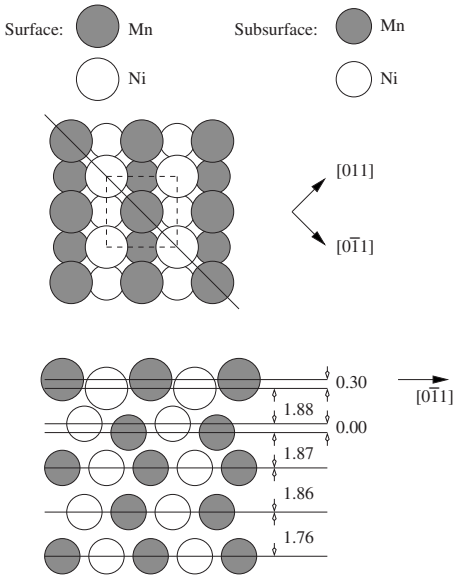

FIG. 1. Structural model of Mn-Ni bulk alloy. (a) Overview, where the unit cell is set by the square in doted lines. (b) Interplanar distances obtained by Wuttig *et al.* (Ref. 11).

III. RESULTS

We have carried out a systematic calculation on the magnetic map of the following systems, in equilibrium geometry: (i) clean Ni surface; (ii) Mn monolayer; (iii) Mn-Ni surface alloy; and (iv) the bilayer surface alloy on a Ni substrate. Calculations have been done in the collinear approach.

A. Clean Ni surface

Magnetic moments (in μ_B) and Δz interlayer spacings (Å) with respect to the previous layer located in the bottom, are

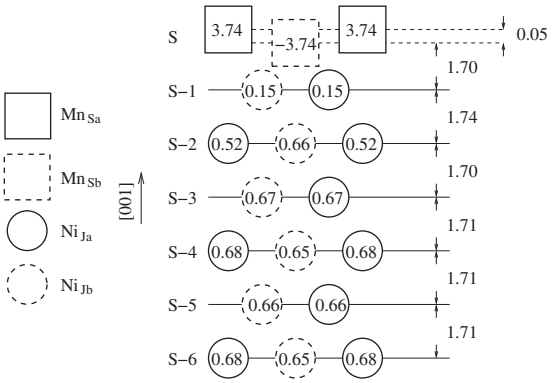

FIG. 2. Magnetic moments (in μ_B) and equilibrium geometry of a Mn overlayer on Ni/Cu(001). There are two inequivalent atoms on each layer. "S-6" is the center of Ni film with 11 planes. S is the surface plane containing the Mn atoms. Magnetic moments of each atom are in circles and squares, in dashed and solid lines. Interplane distances are given in Å. J=S-1,...,S-6.

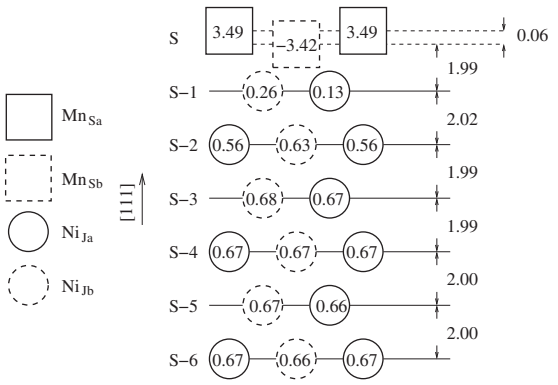

FIG. 3. Magnetic moments (in μ_B) and equilibrium geometry of a Mn overlayer on Ni/Cu(111). There are two inequivalent atoms on each layer. S-6 is the center of Ni film with 11 planes. S is the surface plane containing the Mn atoms. Magnetic moments of each atom are in circles and squares, in dashed and solid lines. Interplane distances are given in Å. J=S-1,…,S-6. Ni_{2a} *and* Ni_{2b} atoms experience a different environment in (111) crystallographic face and this explains why they have different magnetization.

compiled in Table I, in the case of a clean Ni surface for [001], [111], and [011] crystallographic directions, respectively. The clean Ni surface presents a contraction of the first surface plane with 1.64, 1.97, and 1.07 Å for the interlayer distance between the surface and the subsurface, respectively, for (001), (111), and (011) faces. The interlayer distance at the center of the substrate is of 1.71, 2.01, and 1.23 Å for (001), (111), and (011) crystallographic faces, respectively. The intrinsic ferromagnetic coupling of Ni is clearly shown for these three faces. The Ni atoms at the surface exhibit a high magnetic moment [$0.75\mu_B$ for the (001) face, $0.71\mu_B$ for the (111) face, and $0.81\mu_B$ for the (011) face] compared to those obtained at the center of the Ni substrate [$0.65\mu_B$ for the (001) face, $0.66\mu_B$ for the (111) face, and $0.64\mu_B$ for the (011) face]. The enhancement of the magnetic moment at the Ni top layer is clear as expected.

This enhancement is due to the Ni band narrowing at the surface and is similar to that found on the (001) surface of

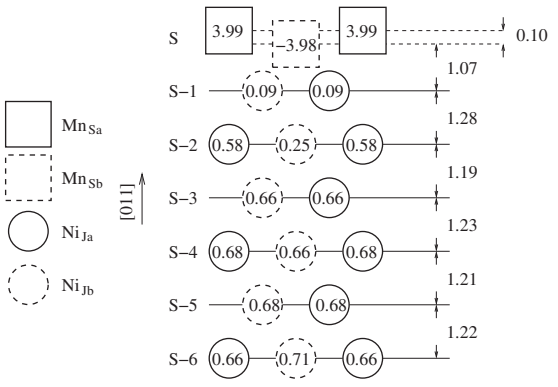

FIG. 4. Magnetic moments (in μ_B) and equilibrium geometry of a Mn overlayer on Ni/Cu(011). There are two inequivalent atoms on each layer. S-6 is the center of Ni film with 11 planes. S is the surface plane containing the Mn atoms. Magnetic moments of each atom are in circles and squares, in dashed and solid lines. Interplane distances are given in Å. J=S-1,…,S-6.

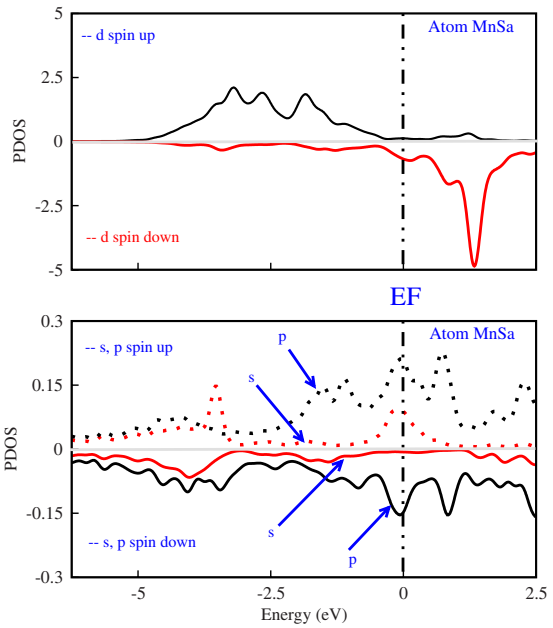

FIG. 5. (Color online) *s*, *p*, and *d* spin-up and spin-down orbital projected density of states of Mn_{Sa} atom on the S surface plane of the system consisting of a Mn monolayer deposited on Ni(001), (see Fig. 2). The Fermi level (E_F) is set at 0. Note the scale difference between "*sp*" and "*d*" states.

Ni.[22,23] This predicted large inward relaxation at the surface is in qualitative agreement with Spišák and Hafner results[22] but contrasts with the weak outward relaxation deduced from LEED experiment[24] or with the homogeneous fcc structure of the Ni films found in the more recent work.[25] Possible

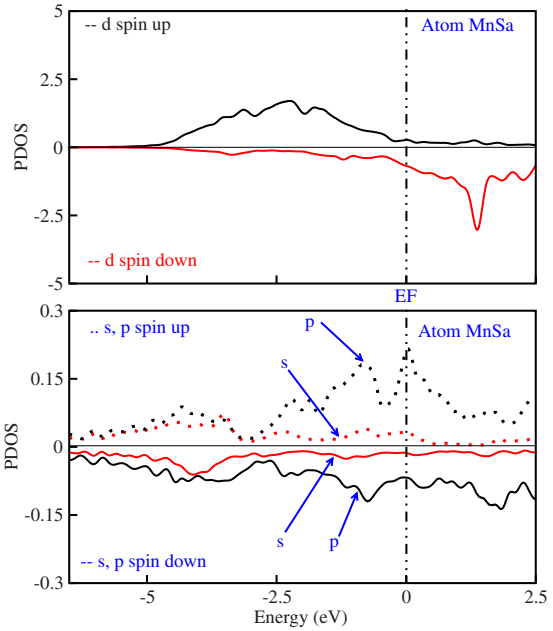

FIG. 6. (Color online) *s*, *p*, *and d* spin-up and spin-down orbital projected density of states of Mn_{Sa} atom on the S surface plane of the system consisting of a Mn monolayer deposited on Ni(111), (see Fig. 3). The Fermi level (E_F) is set at 0. Note the scale difference between *sp* and *d* states.

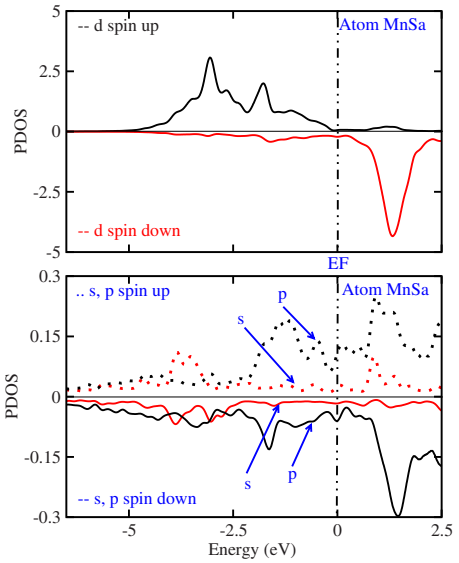

FIG. 7. (Color online) *s*, *p*, *and d* spin-up and spin-down orbital projected density of states of Mn_{Sa} atom on the S surface plane of the system consisting of a Mn monolayer deposited on Ni(011), (see Fig. 4). The Fermi level (E_F) is set at 0. Note the scale difference between *sp* and *d* states.

sources of the disagreement was discussed by Spišák and Hafner.[22] It was concluded that there is a surfactant effect during the formation of the Ni films on Cu(001) and that the surfactant effect eliminates the discrepancy between theory and LEED experiments.

B. Mn monolayer on a Ni substrate

Magnetic moments (in μ_B) and Δz interlayer spacings (Å) with respect to the previous layer located in the bottom, are compiled in Figs. 2–4, in the case of a Mn ML on Ni for [001], [111], and [011] crystallographic directions, respectively.

For (001), (111), and (011) crystallographic faces a much more complex result appears in a Mn ML on fcc Ni; half of the Mn atoms noted Mn_{Sb} are located at 1.70, 1.99, and 1.07 Å for (001), (111), and (011), respectively, from the Ni subsurface layer. The other half of Mn_{Sa} atoms are strongly pushed outward; they are located at 0.05, 0.06, and 0.10 Å for (001), (111), and (011), respectively, from the Mn_{Sb} atoms. On these figures three facts are clearly shown: (i) the Mn monolayer on Ni presents a clear antiferromagnetic behavior for (001), (111), and (011) faces; (ii) the magnetic moments on the Ni atoms in the subsurface layer are clearly depressed; and (iii) the magnetic moments on the two types of Mn atoms are almost equal in magnitude [$3.74\mu_B$ and $-3.74\mu_B$ for (001), $3.49\mu_B$ and $-3.42\mu_B$ for (111), and $3.99\mu_B$ and $-3.98\mu_B$ for (011)]. We have noted that Mn atoms with positive (negative) magnetic moment are pushed outward (inward) for (001), (111), and (011) crystallographic faces. It must be remembered here that bulk Mn is of anti-

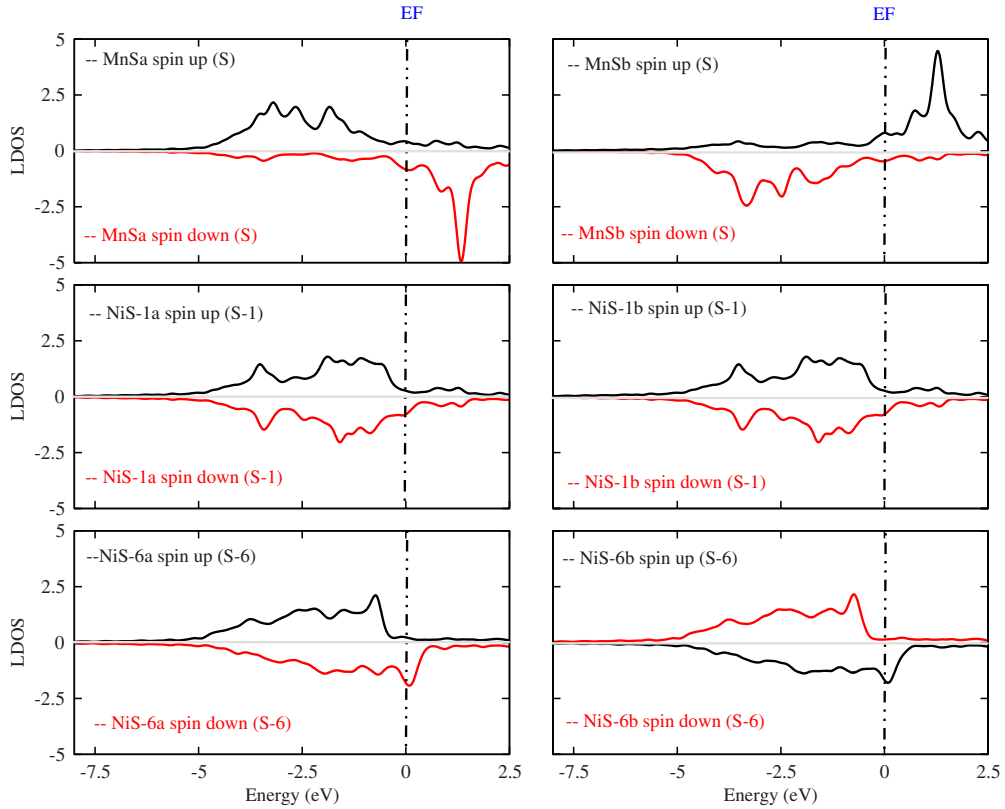

FIG. 8. (Color online) Local spin density of states up and down of Mn_{Sa} and Mn_{Sb} on S plane, $Ni_{S\text{-}1a}$ and $Ni_{S\text{-}1b}$ on "S-1" plane, and $Ni_{S\text{-}6a}$ and $Ni_{S\text{-}6b}$ on S-6 plane, of the system consisting of a Mn monolayer deposited on Ni(001), (see Fig. 2). The Fermi level (E_F) is set at 0.

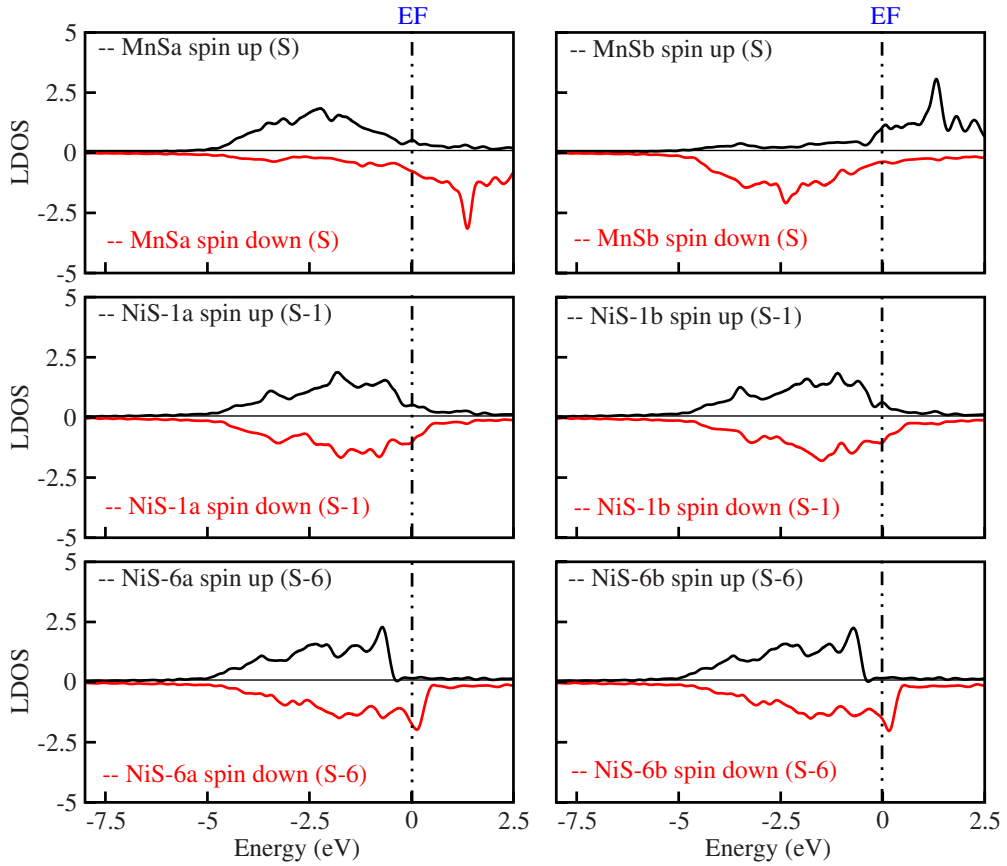

FIG. 9. (Color online) Local spin density of states up and down of Mn_{Sa} and Mn_{Sb} on S plane, $Ni_{S\text{-}1a}$ and $Ni_{S\text{-}1b}$ on S-1 plane, and $Ni_{S\text{-}6a}$ and $Ni_{S\text{-}6b}$ on S-6 plane, of the system consisting of a Mn monolayer deposited on Ni(111), (see Fig. 3). The Fermi level (E_F) is set at 0.

ferromagnetic type[26–28] and thus, in principle, a Mn monolayer should present a purely antiferromagnetic behavior. On the other hand, Mn is in contact with Ni which is a strong ferromagnet; thus a strong induced polarization of Mn by the Ni substrate is present. These two effects (antiferromagnetic bulk Mn and Ni induced ferromagnetism) compete and lead to the behavior displayed in Figs. 2–4. Moreover, as discussed by Hafner and Spisak,[26] in the case of Mn monolayer on Fe(100) these two effects lead to noncollinearity in the Mn overlayer. It is clearly shown that the magnitude of the antiferromagnetic coupling found here depends on crystallographic faces.

It is to notice that, in the case of Mn monolayer on Ni(001) face, the metastable solution with FM coupling between Mn inequivalent atoms has an energy (per supercell used in the present simulation) that is 0.19 Ry higher than the AF genuine ground state. The relaxed FM state presents a total force that is lower than the AF one by 0.8 mRy/a.u. The magnetic moments on the two types of Mn is dramatically different ($3.38\mu_B$ and $0.58\mu_B$). By using XMCD measurements, O'Brien and Tonner[16] predicted a ferromagnetic coupling for the Mn monolayer on Ni(001).

The Mn overlayer on fcc Ni(001) exhibits an AF coupling between Mn inequivalent atoms with enhanced magnetization from both Mn inequivalent atoms (cf. Figs. 2, 5, and 8). The magnetic moments of Ni atoms in the S-1 subsurface plane are smaller than the magnetic moments of Ni atoms in the other subsurface planes. This magnetic behavior is observed also in (111) and (011) faces [cf. Fig. 3 for (111) face and Fig. 4 for (011) face]. It can be explained by the coupling of $Ni_{S\text{-}1}$ atoms with the Mn atoms at the surface that presents magnetic moments oriented in opposite directions.

Figures 5–7 show the PDOS of Mn_{Sa} atom on the "S" surface plane for (001), (111), and (011) faces, respectively. For (001) face, around the Fermi level (E_F), the electronic spectrum of PDOS is entirely dominated by $3d$ states. The s orbitals contribute to tail at high binding energies and to the peak at about −3.5 eV for the majority-spin states. The p states merely produce a low, structureless background to the $3d$ DOS extending from −5 eV up to E_F. For (111) and (011), similar observations have been shown, i.e., the contribution of d electrons is more important than the s and p ones. The local density of states (LDOS) is drawn in Figs. 8–10 for (001), (111), and (011) faces, respectively, for the majority- and minority-spin contributions. A simple analysis reflects the different character of Mn atoms occupying the crystallographically inequivalent sites and reveals drastic differences in the local electronic structure. For (001), (111), and (011) faces, while the LDOS from the Mn_{Sa} majority-spin states is strongly structured and displays a deep minimum at the Fermi energy, that from the Mn_{Sa} minority-spin states one shows rather little structure. On the Mn_{Sa} sites carrying the largest magnetic moments we find an almost completely filled majority d band and a strongly depleted minority band. However, for the Mn_{Sb} atoms, while the LDOS from minority-spin states is strongly structured and displays a

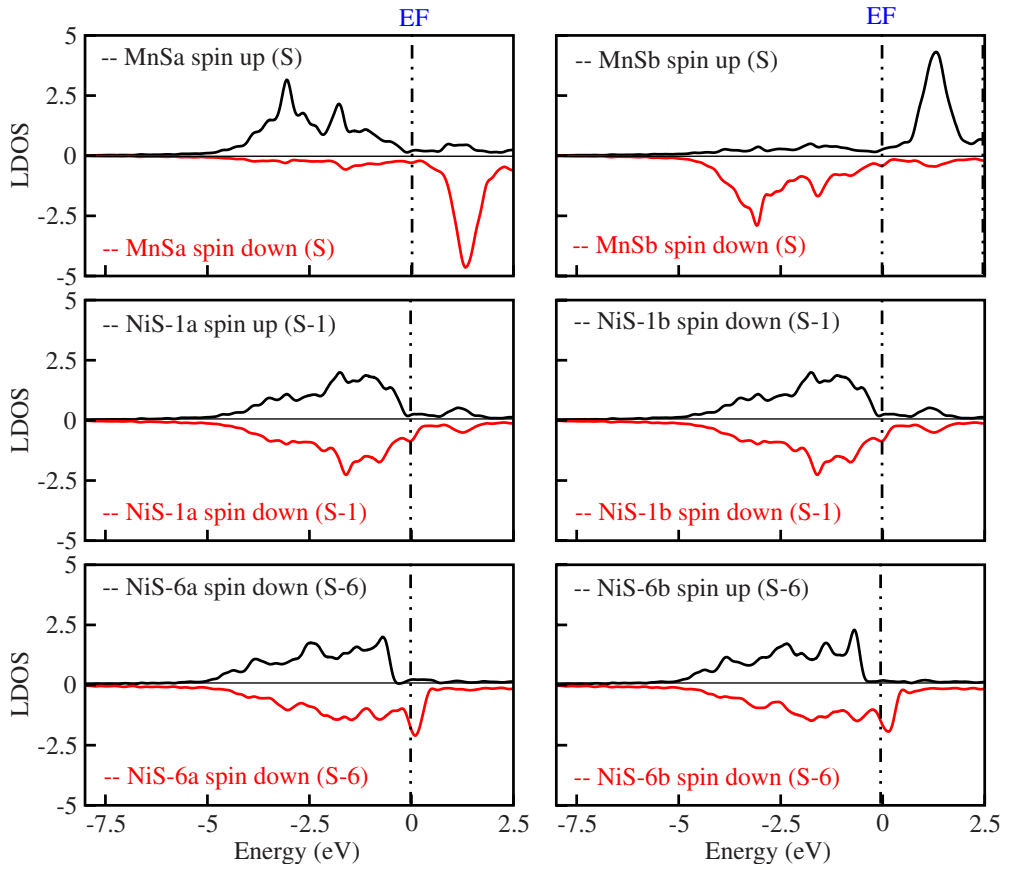

FIG. 10. (Color online) Local spin density of states up and down of Mn_{Sa} and Mn_{Sb} on S plane, $Ni_{S\text{-}1a}$ and $Ni_{S\text{-}1b}$ on S-1 plane, and $Ni_{S\text{-}6a}$ and $Ni_{S\text{-}6b}$ on S-6 plane, of the system consisting of a Mn monolayer deposited on Ni(011), (see Fig. 4). The Fermi level (E_F) is set at 0.

deep minimum at E_F, that from majority-spin states one shows rather little structure, compared to the Mn_{Sa} LDOS. On the Mn_{Sb} sites carrying the largest magnetic moments, but opposite in magnitude to Mn_{Sa} ones, we find an almost completely filled spin-down *d* band and a strongly depleted spin-up *d* band. The AF coupling between Mn overlayer atoms and the fact that Mn atoms are strongly magnetized are clearly exhibited for (001), (111), and (011) faces (cf. Figs. 8–10).

C. Mn-Ni surface alloy on a Ni substrate

Magnetic moments (in μ_B) and Δz interlayer spacings (Å) with respect to the previous layer located in the bottom, are compiled in Figs. 11–13, in the case of a Mn-Ni ordered alloy one-layer thick on Ni for [001], [111], and [011] crystallographic directions.

For (001) face, an atomic corrugation at the surface plane is shown; Ni atoms noted Ni_{Sb} are located at 1.70 Å from the Ni subsurface layer whereas Mn atoms noted Mn_{Sa} are strongly pushed outward. These Mn atoms are located at 0.26 Å from the Ni_{Sb} atoms (cf. Fig. 11). For (111) face, an atomic corrugation at the surface plane is shown; Ni atoms noted Ni_{Sb} are located at 1.96 Å from the Ni subsurface layer whereas Mn atoms noted Mn_{Sa} are strongly pushed outward. These Mn atoms are located at 0.14 Å from the Ni_{Sb} atoms (cf. Fig. 12). For (011) face, an atomic corrugation at the surface plane is shown; Ni atoms noted Ni_{Sb} are located at 1.08 Å from the Ni subsurface layer whereas Mn atoms noted Mn_{Sa} are strongly pushed outward. These Mn atoms are located at 0.25 Å from the Ni_{Sb} atoms (cf. Fig. 13). In Figs. 11–13 three facts are shown: (i) the Mn-Ni ordered alloy one-layer thick on Ni presents a ferromagnetic

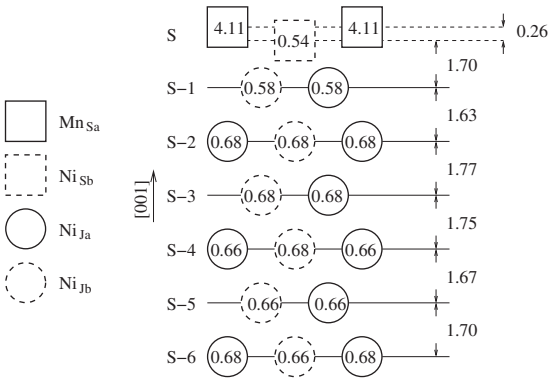

FIG. 11. Magnetic moments (in μ_B) and equilibrium geometry of 1 ML Mn-Ni ordered alloy monolayer on Ni/Cu(001). There are two inequivalent atoms on each layer. S-6 is the center of Ni film with 11 planes. S is the surface plane containing the Mn-Ni ordered alloy atoms. Magnetic moments of each atom are in circles and squares, in dashed and solid lines. Interplane distances are given in Å. J=S-1, . . . ,S-6.

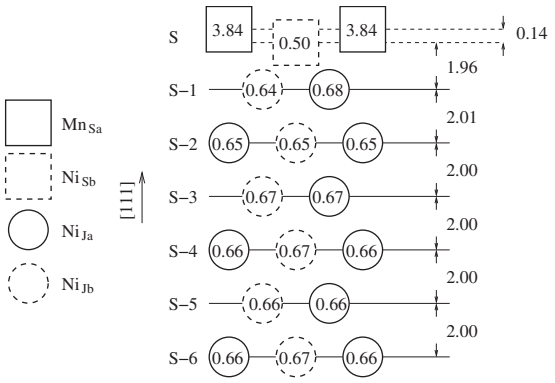

FIG. 12. Magnetic moments (in μ_B) and equilibrium geometry of 1 ML Mn-Ni ordered alloy monolayer on Ni/Cu(111). There are two inequivalent atoms on each layer. S-6 is the center of Ni film with 11 planes. S is the surface plane containing the Mn-Ni ordered alloy atoms. Magnetic moments of each atom are in circles and squares, in dashed and solid lines. Interplane distances are given in Å. J=S-1,...,S-6.

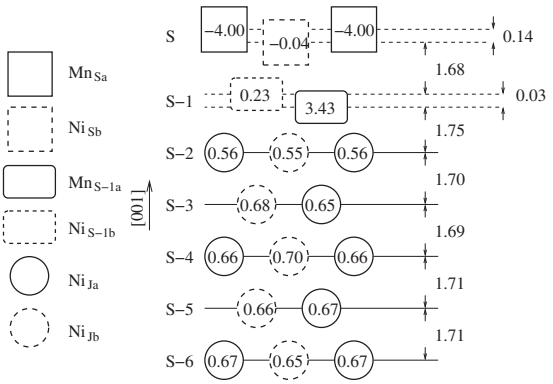

FIG. 14. Magnetic moments (in μ_B) and equilibrium geometry of 2 ML Mn-Ni ordered alloy on Ni/Cu(001). There are two inequivalent atoms on each layer. S-6 is the center of Ni film with nine planes. S and S-1 are the surface and subsurface plane, respectively, containing the Mn and Ni atoms. Magnetic moments of each atom are in circles and squares, in dashed and solid lines. Interplane distances are given in Å. J=S-2,...,S-6.

coupling; (ii) Ni atoms noted Ni_{Sb} are reduced magnetic moments than Ni atoms in other planes for (001) and (111) faces, and (iii) Mn atoms are in the high-spin state [4.11μ_B, 3.84μ_B, and 4.14μ_B, respectively, for (001), (111), and (011) faces].

For (001), (111), and (011) crystallographic faces the Mn-Ni alloy 1 ML on Ni exhibits a FM coupling between Mn and Ni atoms (cf. Figs. 11–13, respectively). The Mn magnetic moment is large [4.11μ_B, 3.84μ_B, and 4.14μ_B, respectively, for (001), (111), and (011) faces], in good agreement with Bala *et al.*[17] Indeed, they predicted the MLs of Sc, Cr, and Mn to be highly magnetic with fairly large magnetic moment per atom whereas the Ni one is reduced magnetic moment [0.58μ_B and 0.50μ_B, respectively, for (001) and (111) faces] in comparison to the bulk value. This trend is already observed in the case of Mn-Co 1 ML on Co(001) by M'Passi-Mabiala *et al.*[8]

The FM coupling between Mn and Ni atoms, obtained in the present calculations, for (001), (111), and (011) faces, is in good agreement with both magnetic measurements[16] and electron spectroscopy,[11] and with Spišák and Hafner calculated results.[29]

D. Bilayer surface alloy on a Ni substrate

Magnetic moments (in μ_B) and Δz interlayer spacings (Å) with respect to the previous layer located in the bottom, are displayed in Figs. 14–16, in the case of a Mn-Ni ordered alloy two-layers thick on Ni for [001], [111], and [011] crystallographic directions.

For (001) face, a ripple at the surface and subsurface planes is observed. At the subsurface plane, Mn atoms noted $Mn_{S\text{-}1a}$ are located at 1.75 Å from the Ni atoms in S-2 layer whereas Ni atoms noted $Ni_{S\text{-}1b}$ are weakly pushed outward

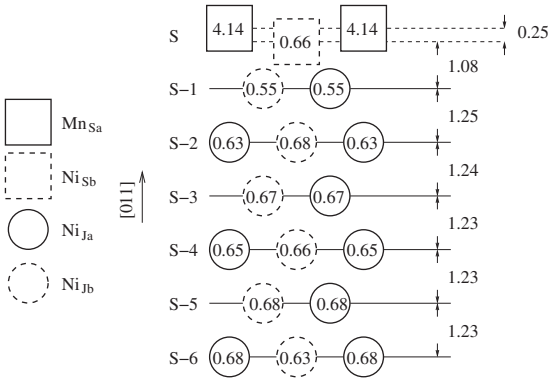

FIG. 13. Magnetic moments (in μ_B) and equilibrium geometry of 1 ML Mn-Ni ordered alloy monolayer on Ni/Cu(011). There are two inequivalent atoms on each layer. S-6 is the center of Ni film with 11 planes. S is the surface plane containing the Mn-Ni ordered alloy atoms. Magnetic moments of each atom are in circles and squares, in dashed and solid lines. Interplane distances are given in Å. J=S-1,...,S-6.

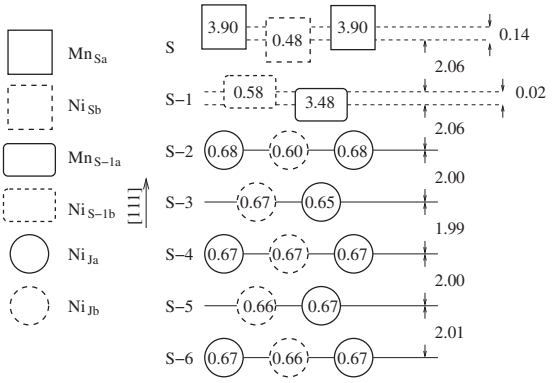

FIG. 15. Magnetic moments (in μ_B) and equilibrium geometry of 2 ML Mn-Ni ordered alloy on Ni/Cu(111). There are two inequivalent atoms on each layer. S-6 is the center of Ni film with nine planes. S and S-1 are the surface and subsurface planes, respectively, containing the Mn and Ni atoms. Magnetic moments of each atom are in circles and squares, in dashed and solid lines. Interplane distances are given in Å. J=S-2,...,S-6.

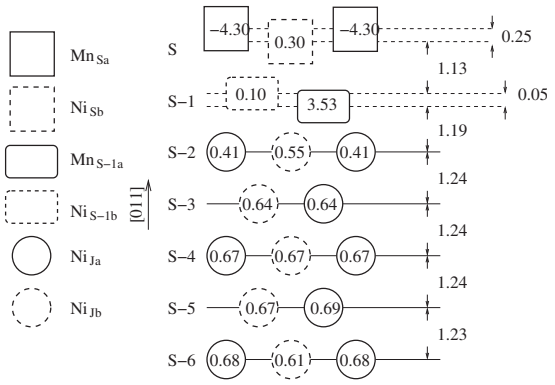

FIG. 16. Magnetic moments (in μ_B) and equilibrium geometry of 2 ML Mn-Ni ordered alloy on Ni/Cu(011). There are two inequivalent atoms on each layer. S-6 is the center of Ni film with nine planes. S and S-1 are the surface and subsurface planes, respectively, containing the Mn and Ni atoms. Magnetic moments of each atom are in circles and squares, in dashed and solid lines. Interplane distances are given in Å. J=S-2,...,S-6.

the surface plane about 0.03 Å from the $Mn_{S\text{-}1a}$ atoms. At the surface plane, Ni atoms noted Ni_{Sb} are located at 1.68 Å from the $Ni_{S\text{-}1b}$ subsurface atoms. Mn atoms noted Mn_{Sa} are strongly pushed outward. These Mn atoms are located at 0.14 Å from the Ni_{Sb} atoms (cf. Fig. 14). Also, we observe: (i) a FM coupling between Mn and Ni atoms in subsurface and surface planes, respectively; (ii) a layered AF sequence is found in the Mn-Ni ordered alloy two-layers thick; (iii) Mn_{Sa} atoms at the surface are in an high-spin state in comparison to the magnetic moments obtained for the $Mn_{S\text{-}1a}$ atoms at the subsurface ($4.00\mu_B$ against $3.43\mu_B$), and (iv) Ni_{Sb} magnetic moments at the surface are killed ($-0.04\mu_B$) whereas at the subsurface $Ni_{S\text{-}1b}$ magnetic moments are weak ($0.23\mu_B$).

For (111) face, a ripple at the surface and subsurface planes is also observed. At the subsurface plane, Mn atoms noted $Mn_{S\text{-}1a}$ located at 2.06 Å from the Ni atoms in S-2 layer whereas Ni atoms noted $Ni_{S\text{-}1b}$ are weakly pushed outward the surface plane about 0.02 Å from the $Mn_{S\text{-}1a}$ atoms. At the surface plane, Ni atoms noted Ni_{Sb} are located at 2.06 Å from the $Ni_{S\text{-}1b}$ subsurface atoms. Mn atoms noted Mn_{Sa} are strongly pushed outward. These Mn atoms are located at 0.14 Å from the Ni_{Sb} atoms (cf. Fig. 15). Also, we observe: (i) a FM coupling between Mn and Ni atoms in subsurface and surface planes, respectively; (ii) a layered FM sequence is found in the Mn-Ni ordered alloy two-layers thick; (iii) Mn_{Sa} atoms at the surface are in an high-spin state in comparison to the magnetic moments obtained for the $Mn_{S\text{-}1a}$ atoms at the subsurface (3.90 against $3.48\mu_B$), and (iv) Ni_{Sb} ($Ni_{S\text{-}1b}$) magnetic moments at the surface, i.e., $0.48\mu_B$ (at the subsurface, i.e., $0.58\mu_B$) are marginally lower as compared to bulk values.

For (011) face, a ripple at the surface and subsurface planes is also observed. At the subsurface plane, Mn atoms noted $Mn_{S\text{-}1a}$ located at 1.19 Å from the Ni atoms in S-2 layer whereas Ni atoms noted $Ni_{S\text{-}1b}$ are weakly pushed outward the surface plane about 0.05 Å from the $Mn_{S\text{-}1a}$ atoms. At the surface plane, Ni atoms noted Ni_{Sb} are located at 1.13 Å from the $Ni_{S\text{-}1b}$ subsurface atoms. Mn atoms noted Mn_{Sa} are strongly pushed outward. These Mn atoms are located at 0.25 Å from the Ni_{Sb} atoms (cf. Fig. 16). Also, we observe: (i) a FM and an AF coupling between Mn and Ni atoms in subsurface and surface planes, respectively; (ii) an AF coupling between Mn atom nearest-neighboring positions is found in the Mn-Ni ordered alloy two-layers thick; (iii) Mn_{Sa} atoms at the surface are in an high-spin state in comparison to the magnetic moments obtained for the $Mn_{S\text{-}1a}$ atoms at the subsurface ($-4.30\mu_B$ against $3.53\mu_B$), and (iv) Ni_{Sb} and $Ni_{S\text{-}1b}$ magnetic moments (at the surface and at the subsurface, respectively) are weak ($0.30\mu_B$ and $0.10\mu_B$, respectively).

The corrugation observed in the case of Mn-Ni ordered alloy one-layer thick is in agreement with experimental results done by Wuttig *et al.*[11] and De Santis *et al.*,[15] for (001) and (011) faces, respectively. The subsurface reveals weak corrugation of Mn atoms. We believe that these transformed structures should be closely related with the magnetic properties of the film surface. As discussed in Ref. 22 at the surface the lower coordination of the atoms leads to a narrowing of the *d* bands and an enhanced moment in magnetic materials. In the Mn surface alloys, this *d*-band narrowing may be increased by outward buckling. It has been shown by Wuttig *et al.*[11] that the strong corrugation of 0.30 ± 0.02 Å found for the Ni(001) $c(2\times2)$Mn surface alloy formed after deposition of 4 ML Mn is due to the enhanced magnetic moment of the Mn atom.

The Mn-Ni ordered alloy two-layers thick on Ni(001) presents a layered AF sequence (cf. Fig. 14) in agreement with previous calculations done by Spišàk and Hafner[29] but at odd with experimental results[16] showing evidence of a FM coupling. Antiferromagnetic coupling between Mn atom nearest-neighboring positions is depicted for (001) and (011) faces. However, the Mn magnetic moment is parallel to Ni one at the interface. Mn magnetic moment is large whereas Ni one is reduced magnetic moment. This small Ni moment is a result of frustration effects.

The formation energy for the 1 ML Mn-Ni alloy calculated by the Blügel formula[30] is about −385, −35, and −31 mRy, respectively, for (001), (111), and (011) crystallographic faces, showing evidence of the surface-alloy formation. We point out that the 2 ML Mn-Ni alloy is more stable than the Mn overlayer by about 250 mRy in the case of (001) face, and by about 58 mRy in the cases of (111) face. Whereas for (011) face, the Mn overlayer is more stable than the 2 ML Mn-Ni alloy by about 22 mRy.

It should be pointed out that the Ni atoms belonging at the top of Ni film [i.e., Ni_{1a} and Ni_{1b} for both 1 ML Mn-Ni ordered alloy and Mn overlayer on Ni/Cu(111) and, Ni_{2a} and Ni_{2b} for 2 ML Mn-Ni ordered alloy on Ni/Cu(111)] experience a different environment in (111) crystallographic face and this explains why they have different magnetization. But this is not the same case with both (001) and (011) crystallographic orientations, where Ni atoms experience a same environment.

IV. DISCUSSION

By assuming that the magnetism of one atom is mainly determined by the interaction with its neighbor atoms (in the

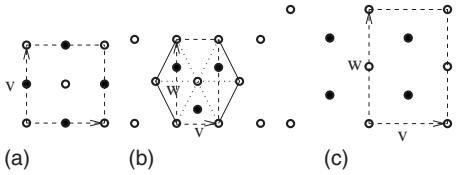

FIG. 17. Schema representing basis vectors (v and w of the supercell in the x-y plane. (a) For (001) face with $v=a_{Cu}$; (b) for (111) face with $v=a_{Cu}/\sqrt{2}$ and $w=\sqrt{\frac{3}{2}}a_{Cu}$; and (c) for (011) face with $v=a_{Cu}$ and $w=a_{Cu}/\sqrt{2}$.

following discussion, the term FM or AF coupling of an atom with another is intended with one of its neighbors, also if the term "neighbors" is omitted), we can infer from the data we obtained the following rules, that can explain, at least qualitatively, all our results.

In general, we have: (i) Ni atom couples ferromagnetically (FM) with a neighbor Ni atom; (ii) Mn atom couples FM with a neighbor Ni atom but antiferromagnetically with a neighbor Mn atom; (iii) in the case where the above rules generate a "conflict of interest" (COI), (i.e., an atom couple FM with some neighbor but AF with other neighbors), the atom tends to reduce the magnetization; (iv) the magnetization of the atom follows, as a first (and very rough) approximation, the magnetic orientation of the majority of neighbors, but, in addition to this "majority rule," the magnetization is also strongly influenced by the distance, the number, and the symmetry arrangement of the neighbors.

We recall that, for each substrate orientation, the unit cell considered is made of two atoms per layer, that are labeled a and b. However, different geometries and different neighbors arrangements correspond to different orientations (see Fig. 17).

The (001) surface presents the more symmetric arrangement: each a (b) atom at the surface has in the surface layer (hereafter denoted as the S layer) four b (a) atoms as neighbors, at a distance $a_{Cu}/\sqrt{2}$, and four a (b) atoms as next-nearest neighbor at a distance a_{Cu} while the same a (b) surface atom has in the subsurface (hereafter denoted as the S-1) layer, two a and two b atoms as neighbors.

The (011) surface has a less symmetric arrangement; each a (b) atom at the surface (S layer) has in the surface layer (S layer) two b (a) atoms as nearest neighbors (at distance $a_{Cu}/\sqrt{2}$) and two a (b) atoms at slightly larger distance (a_{Cu}). As for the (001) case, an a (b) atom at the (011) surface has in the subsurface (S-1) layer two a and two b atoms as neighbors.

The (111) surface presents a quite a different situation; each a (b) atom at the surface has six nearest neighbors: two of them are a (b) and four of them are b (a). The a (b) atom at the surface has only three neighbors in the subsurface layer; two are b (a) atoms one is a a (b) atom.

With this in mind we can try to explain the difference in the magnetization in the three surfaces.

A. Ni clean surface and Mn-Ni monolayer

The cases of Ni clean surfaces and the surfaces with a Ni-Mn monolayer considered in the present work are straightforward since there are no Mn-Mn neighbors, no atom presents COI, and all atoms are FM coupled. In fact, all the three orientations of the slabs present the same behaviors (see, Table I and Figs. 11–13), with small differences in the magnetization of surface atoms that can be explained by the different distances between the surface and the subsurface layers; the magnetization of Mn (or Ni) surface atom decreases as the interlayer distance increases.

B. Mn monolayer

The three cases of Mn surface monolayer are more complexes since Mn tends to couple AF with the other Mn atom but FM with the substrate. For simplicity, in the following, we discuss only the case of a atoms in the surface or subsurface layers when the same discussion can be straightforwardly applied to the case of b atom (in general, by simple exchanging the label $a \leftrightarrow b$).

In the case of (011) surface, each Mn_{Sa} atom has, in the surface layer, as neighbors two b atoms at the distance $a_{Cu}/\sqrt{2}$ (while the other two a atoms are at a_{Cu}), the AF interaction prevails and the Mn_{Sa} atom is AF coupled with the Mn_{Sb} atom; the absolute value of the magnetic moment of Mn atom on (011) surface is larger than the magnetic moment presented by Mn atoms on the (001) and (111) substrates. For the (011) orientation, the subsurface Ni atoms present a COI since they have two Mn neighbor atoms at the surface that present a FM moment and two other Mn neighbor surface atoms with AF moments. As a consequence, the Ni_{S-1} atoms reduce their magnetic moments up to a negligible value.

In the case of Mn monolayer on the Ni (111) surface a majority law apply: the energetically favored configuration is the one with AF coupling of Mn a and b atoms, which produces an arrangement where a Mn atom has, as nearest neighbors, four Mn atoms in the AF configuration and only two FM Mn atoms. In the subsurface S-1 layer the Ni atoms are FM coupled with the others Ni but the peculiar symmetry of this orientation produce an important difference: one Ni_{S-1b} atom has as neighbors in the surface layer two FM Mn a atoms and one AF Mn b atom, and, according to the majority law, presents a magnetic moment that is reduced with respect to the bulk value (due to the COI with the Mn b atom), but it is still significant, $\sim 0.26\mu_B$. For the other Ni_{S-1a} atom, the COI is more pronounced since Ni_{S-1a} has as neighbors in the surface layer one FM Mn a atom and two AF Mn b atoms; as a consequence, the magnetic moment of Ni_{S-1a} atom is only $\sim 0.13\mu_B$, i.e., one half of the magnetic moment of the Ni_{S-1b} atom.

Finally, we discuss the case of a Mn monolayer on Ni(001) substrate, that is, similar to the case of the two orientations discussed above. The Mn_{Sa} (Mn_{Sb}) atom at the surface has four nearest neighbors Mn_{Sb} (Mn_{Sa}) atoms and it is coupled AF with them according to the general rule (ii). Ni atoms in the subsurface layer are coupled FM with all Ni neighbor atoms in the S-1 and in the S-2 layers but they are in COI with the Mn atoms of the surface: the Ni_{S-1a} (Ni_{S-1b}) atoms are coupled FM with two neighbors Mn atoms at the surface and AF with the two other neighbors Mn atoms at the

surface. As a consequence the Ni_{S-1} atoms tend to reduce their magnetic moments according to rule (iii) and to present a magnetization oriented as the substrate according to rule (iv). For the case of Mn monolayer, we note that the absolute magnetization on Mn_S atoms on (001) substrate is intermediate with respect to the absolute magnetization Mn_S on different oriented substrates considered and the magnetization of Ni_{S-1} atoms on (001) substrate is also intermediate with respect to the average of the magnetization of Ni_{S-1} on (011) and on (111) substrates. These trends confirm the validity of the qualitative rules (i)–(iv) states at the beginning of this section.

C. Mn-Ni bilayer

The case of Mn-Ni bilayer is less straightforward since in some cases, there are atoms presenting the COI. According to the rules exposed above, in the case of a Mn-Ni bilayer, the Mn atom at the subsurface tends to couple FM with the Ni atoms in the S-1 and S-2 layers, for all the three orientations considered, as can be noticed looking to Figs. 14–16, where the data relative to the three surface orientations are displayed. In the case of (001) and (011) substrates, the Mn at S-1 couples AF with the two surface Mn neighbor atoms [rule (ii)]. The surface Ni is in COI since it tends to couple FM with two surface Mn with magnetic moment down and to couple FM with the four subsurface atoms (two Mn and two Ni) with magnetic moment up. As a result, the magnetic moment of Ni is reduced [about one half for the (011) surface] or becomes negligible [for the (001) surface], according to rule (iii). For (111) orientation, the Mn subsurface atom has, as neighbors in the surface layer, two Ni atoms and one Mn atom; according the majority rules the FM interaction with the two Ni_S atoms prevails (in fact, the Ni_S atom has the larger magnetic moment with respect to the other Ni_S atoms on substrates with different orientations, displayed in Figs. 14 and 16). Considering only the interaction with the neighbors, now, each surface Mn_{Sa} atom is coupled FM with four surface Ni and with two subsurface Ni while it is coupled AF only with one subsurface Mn (and FM with two neighbor Mn_{Sa} atoms according to the symmetry of the unit cell chosen). According to the majority rule [i.e., rule (iv)] the FM coupling prevails, explaining the results displayed in Figs. 14–16.

V. SUMMARY

We have reported on, by using the *ab initio* techniques, a systematic study of structural and magnetic properties of Mn/Ni system grown epitaxially on Cu substrate, in crystallographic faces with Low-Miller indices, using the spin-polarized calculations within the density-functional approach of Kohn and Sham, with generalized gradient approximation, by the pseudopotential PWSCF code. We have found, for (001) face, an AF coupling for Mn overlayer on Ni with large magnetic moments ($3.74\mu_B$ and $-3.74\mu_B$) in both inequivalent Mn atoms. The Ni subsurface atoms adjacent to Mn surface atoms are equivalent and reduced magnetic moments than those values obtained for other subsurface planes. Structural relaxation has shown that the half of Mn atoms (with large magnetic moment) are pushed outward whereas the other half one (with less magnetic moment) are pushed inward, in qualitative agreement with Zenia *et al.*[18] results.

The 1 ML surface alloy has shown a FM coupling between Mn and Ni surface atoms, with a large magnetic moment ($4.11\mu_B$) on Mn sites. An atomic corrugation at the surface is shown, where Mn (Ni) surface atoms are pushed outward (inward), in qualitative agreement with experimental measurements.[11] About 2 ML surface alloy, a layered AF sequence and an AF coupling between Mn atom nearest-neighboring positions are obtained. The Mn (Ni) surface atoms are large (less) magnetic moment ($-4.00\mu_B$ and $-0.04\mu_B$, respectively). A large buckling on Mn atoms is always obtained.

The influence of crystallographic faces on above structural and magnetic properties is also the key point in the present work. For (111) and (011) faces, AF coupling is found for Mn overlayer on Ni with an enhanced magnetic moment from both Mn inequivalent atoms. The Mn atom shows a large polarization [$3.84\mu_B$ and $4.14\mu_B$, respectively, for (111) and (011) faces] with, a FM coupling with Ni atoms in the case of 1 ML surface alloy on Ni. Mn surface-alloy atoms are strongly pushed outward, in agreement with De Santis *et al.*[15] results. In the case of 2 MLs surface alloy, a layered FM sequence is obtained for (111) face whereas an AF coupling between Mn atom nearest-neighboring positions are found for (011) face. We have also noted a rippling at the surface with Mn atoms showing a strong outward.

ACKNOWLEDGMENTS

B.R. Malonda-Boungou would like to address thanks to the AIEA/ICTP STEP-programme for financing this work at the Abdus Salam ICTP. This work is partially supported by the ICTP through the Grant No. OEA-AC-71. Calculations in this work have been done using the plane-wave self-consistent field (PWSCF) code, distributed with the QUANTUM ESPRESSO package.[10] We acknowledge the "Consorzio interuniversitario per le Applicazioni di Supercalcolo Per Universitá e Ricerca" (CASPUR) for computational resources provided under the project "Electronic and magnetic properties on Mn-based materials and nanostructures." We thank R. Martin for a critical reading of the manuscript.

*Corresponding author; malonda_brice@yahoo.fr

[1] C. A. F. Vaz, J. A. C. Bland, and G. Lauhoff, Rep. Prog. Phys. **71**, 056501 (2008), and references therein.
[2] C. Demangeat and J. C. Parlebas, Rep. Prog. Phys. **65**, 1679 (2002).
[3] A. Vega, J. C. Parlebas, and C. Demangeat, *Handbook of Magnetic Materials*, edited by K. H. J. Buschow (Elsevier, New York, 2003), Vol. 15, p. 199.
[4] W. L. O'Brien and B. P. Tonner, Phys. Rev. B **50**, 2963 (1994).
[5] B.-Ch. Choi, P. J. Bode, and J. A. C. Bland, Phys. Rev. B **59**, 7029 (1999).
[6] Yuet-Loy Chan, Jo-Hsuan Sun, Chao-Huang Chen, S. C. Wang, Y. J. Hsu, and D. H. Wei, *Proceedings of Eighth International Conference on X-Ray Microscopy*, IPAP Conference Series Vol. 7 (IPAP, 2005), p. 300.
[7] S. Meza-Aguilar, O. Elmouhssine, H. Dreyssé, and C. Demangeat, Phys. Rev. B **63**, 064421 (2001).
[8] B. M'Passi-Mabiala, S. Meza-Aguilar, and C. Demangeat, Phys. Rev. B **65**, 012414 (2001).
[9] S. Baroni, S. de Gironcoli, A. Dal Corso, and P. Giannozzi, Rev. Mod. Phys. **73**, 515 (2001).
[10] S. Baroni, A. Dal Corso, S. de Gironcoli, and P. Giannozzi, http://www.pwscf.org
[11] M. Wuttig and C. C. Knight, Phys. Rev. B **48**, 12130 (1993).
[12] D. Schmitz, O. Rader, C. Carbone, and W. Eberhardt, Phys. Rev. B **54**, 15352 (1996).
[13] O. Rader, W. Gudat, C. Carbone, E. Vescovo, S. Blügel, R. Kläsges, W. Eberhardt, M. Wuttig, J. Redinger, and F. J. Himpsel, Phys. Rev. B **55**, 5404 (1997).
[14] O. Rader, T. Mizokawa, A. Fujimori, and A. Kimura, Phys. Rev. B **64**, 165414 (2001).
[15] M. De Santis, V. Abad-Langlais, Y. Gauthier, and P. Dolle, Phys. Rev. B **69**, 115430 (2004).
[16] W. L. O'Brien and B. P. Tonner, Phys. Rev. B **51**, 617 (1995).
[17] A. Bala and T. Nautiyal, J. Magn. Magn. Mater. **320**, 2201 (2008).
[18] H. Zenia, S. Bouarab, J. Ferrer, and C. Demangeat, Surf. Sci. **564**, 12 (2004).
[19] M. A. Khan, J. Phys. Soc. Jpn. **62**, 1682 (1993).
[20] D. Vanderbilt, Phys. Rev. B **41**, 7892 (1990).
[21] J. P. Perdew, Y. Wang, and E. Engel, Phys. Rev. Lett. **66**, 508 (1991).
[22] D. Spišák and J. Hafner, J. Phys.: Condens. Matter **12**, L139 (2000).
[23] F. Mittendorfer, A. Eichler, and J. Hafner, Surf. Sci. **423**, 1 (1999), and references cited therein.
[24] S. Müller, B. Schulz, G. Kostka, M. Farle, K. Heinz, and K. Baberschke, Surf. Sci. **364**, 235 (1996).
[25] W. Platow, U. Bovensiepen, P. Poulopoulos, M. Farle, K. Baberschke, L. Hammer, S. Walter, S. Müller, and K. Heinz, Phys. Rev. B **59**, 12641 (1999).
[26] J. Hafner and D. Spišák, Phys. Rev. B **72**, 144420 (2005).
[27] F. Schiller, S. V. Halilov, and C. Laubschat, J. Phys.: Condens. Matter **17**, 3153 (2005).
[28] O. Eriksson, A. M. Boring, R. C. Albers, G. W. Fernando, and B. R. Cooper, Phys. Rev. B **45**, 2868 (1992).
[29] D. Spišàk and J. Hafner, J. Phys.: Condens. Matter **11**, 6359 (1999).
[30] S. Blügel, Appl. Phys. A: Mater. Sci. Process. **63**, 595 (1996).